

# Parallel 3D Hybrid Continuum/DSMC Method for Unsteady Expansions into a Vacuum

Bénédicte D. Stewart<sup>1</sup>

*The University of Texas at Austin, Austin, Tx, 78712*

Elizabetta Pierazzo<sup>2</sup>

*Planetary Science Institute, Tucson, Az, 85719*

*and*

David B. Goldstein<sup>3</sup>, Philip L. Varghese<sup>4</sup>, Laurence M. Trafton<sup>5</sup> and Chris H. Moore<sup>6</sup>

*The University of Texas at Austin, Austin, TX 78712*

We present the application of a unidirectional unsteady coupling between a continuum solver and a three dimensional parallel Direct Simulation Monte Carlo (DSMC) code. Two different problems have been considered: the spherically symmetric expansion of a water vapor cloud into a vacuum and the late stages of a comet impact on the Moon. In both cases, unsteady data pre-computed from a continuum solution are used as input to the DSMC code at a fixed interface. The DSMC results were then compared to the continuum results downstream of the interface in a region of mutual validity in order to validate our approach. The DSMC results for the expansion flow showed good agreement with the analytic solution for the density, velocity and temperature downstream of the interface. Similarly, for the comet impact simulations, the DSMC density agrees well with the solution from the continuum solver, the SOVA hydrocode. A slightly hotter solution is however obtained downstream of the interface using the DSMC code compared to the hydrocode solution.

## Nomenclature

$A, B$	=	constants
$e_{v,i}$	=	specific vibrational energy associated with the $i^{\text{th}}$ mode
$\eta$	=	radial distance from the center of the planet
$F_{ACCEPTED}$	=	estimated fraction of accepted collisions in a cell during a given timestep
$\Gamma$	=	gamma function
$\gamma$	=	ratio of specific heats
$M$	=	mass of the gas
$M_V$	=	number of vibrational modes
$N$	=	number of molecules
$N_k$	=	number of molecules in the $k^{\text{th}}$ excited vibrational level
$N_{ACCEPTED}$	=	number of accepted collision pairs
$N_{SELECT}$	=	number of selected collision pairs (Bird <sup>1</sup> Eq. (11.3))
$N_{TR}$	=	limited number of collisions sufficient for the equilibration of the translational and rotational modes
$N_{VIB}$	=	additional number of collisions required for the possible equilibration of the vibrational modes
$NUM$	=	number of representative molecules in a cell

---

<sup>1</sup> Research Assistant, Dept. of Aerospace Engineering, larignonb@mail.utexas.edu, Student Member AIAA.

<sup>2</sup> Senior Scientist, Planetary Science Institute, betty@psi.edu.

<sup>3</sup> Professor, Dept. of Aerospace Eng. and Eng. Mechanics, david@cfdlab.ae.utexas.edu, Senior Member AIAA.

<sup>4</sup> Professor, Dept. of Aerospace Eng. and Eng. Mechanics, varghese@mail.utexas.edu, Senior Member AIAA.

<sup>5</sup> Senior Research Scientist, Dept. of Astronomy, lmt@astro.as.utexas.edu.

<sup>6</sup> Research Assistant, Dept. of Aerospace Engineering, chris@cfdlab.ae.utexas.edu, Student Member AIAA.

$v$	=	vibrational mode
$\varphi$	=	azimuthal angle
$Q$	=	total energy of the gas
$R$	=	specific gas constant
$R_0, T_0$	=	initial radius and temperature of the gas cloud
$Rand$	=	random number
$r$	=	distance from the center of the cloud
$\rho, T, u$	=	density, temperature and radial velocity component inside the gas cloud
$t$	=	time
$\Theta$	=	polar angle
$\theta_i$	=	characteristic vibrational temperature
$u_{max}$	=	velocity of the outer layers of the cloud
$Z_{V,i}$	=	collision number for the $i^{\text{th}}$ vibrational mode
$Z_{VMIN}$	=	minimum vibrational collision number

## I. Introduction

THE expansion of a gas into a vacuum undergoes several flow regime changes from continuum to transitional to rarefied to free-molecular. The flow in the continuum region can be modeled using the Navier-Stokes equations but rarefaction effects need to be taken into account away from the high density region. As the flow expands, the average distance between molecular collisions, or mean free path, starts to increase and becomes comparable to, or even larger than, any representative length scale of the problem. Under these conditions, the flow has to be modeled by the Boltzmann equation. Unfortunately this equation cannot generally be solved due to the large number of unknowns and the difficulty of modeling the collision integral. For these reasons, a molecular computational approach is generally considered with the Direct Simulation Monte Carlo (DSMC) method<sup>1</sup> being the most widely utilized. The DSMC method<sup>1</sup> is a statistical molecular approach where the flow is simulated using a number of representative molecules. In fact, for a large number of representative molecules, the DSMC method actually solves the Boltzmann equation<sup>2</sup>. The simulated molecules, each of which represents a large number of real molecules, are moved and then collided in separate successive steps. The macroscopic properties of the flow such as density, temperature and velocity are extracted from the molecular data by sampling and averaging over all the molecules. As with any molecular statistical approach, the level of noise observed in the macroscopic properties obtained with the DSMC method is directly linked to the number of simulated molecules. For that reason, the DSMC method is well suited for steady state flows where time averaging or ensemble averaging over a number of realizations can be used to reduce the noise level of the simulations. The DSMC method can effectively solve flows such as nozzle flows and plume impingement for space applications<sup>3,4</sup>, hypersonic re-entry flows<sup>5</sup> and low density atmospheric flows<sup>6-9</sup>.

The DSMC method can solve flows in any regime, from continuum to free molecular, but due to its computational efficiency the method is mostly used to solve transitional-to-rarefied flows. In the cases where both transitional and continuum regions are present in the computational domain, one way to improve the efficiency of the simulations has been to couple the DSMC code with a continuum solver. For these problems, the continuum regions of the flow are solved using the continuum solver and the non-equilibrium regions where the rarefaction effects cannot be ignored are simulated using the DSMC method. Such hybrid methods are generally used to simulate complex expansion and nozzle flows into hard vacuums or into a rarefied background gas as well as hypersonic flows around re-entry vehicles. Roveda *et al.*<sup>10</sup> used a fully coupled hybrid adaptive discrete velocity ADV-DSMC method to simulate a 2D unsteady pressure-driven slit flow. In their simulations, the majority of the domain is computed using the Euler solver ADV with only a few small embedded regions solved using the DSMC method where required. The time-varying location of the interface between the continuum and transitional regions is calculated based on two separate breakdown parameters: the gradient-length local Knudsen number and the value of Bird's parameter<sup>1</sup>. Their approach uses a fully integrated coupling at the interface between the ADV solver and the DSMC solver so that data can be transferred from either region to the other. At the interface, reservoir cells are used in the DSMC domain to create molecules from the ADV macroscopic data while buffer cells are used to calculate continuum fluxes into the ADV domain from the sampled DSMC molecular data. More recently, Vashchenkov *et al.*<sup>11</sup> used a unidirectional coupling between their Navier-Stokes solver and their DSMC solver to simulate nozzle plumes expanding into vacuum while Papp *et al.*<sup>12</sup> used a similar approach to simulate high-altitude plume flows.

Schwartzentruber *et al.*<sup>13</sup> simulated the 2D steady hypersonic flow around a cylinder using a fully coupled hybrid method. In their method, the interface between the two regions is determined using a gradient-length Knudsen number and data are transferred across the interface in a way similar to Roveda *et al.*<sup>10</sup>. Overlap cells again are used at the interface but an additional temporal averaging of the DSMC data is used to reduce the statistical scatter in the boundary conditions for the Navier-Stokes solver.

Hybrid CFD-DSMC methods are used to reduce the cost of the simulations of high density flows with non-equilibrium regions by simulating the regions of the flow in thermal equilibrium using a CFD solver. An alternative way used to simulate the regions of the flow in thermal equilibrium has been to implement a modified DSMC method using a collision-limiting scheme<sup>14, 15</sup>. In the high density regions, a larger timestep and cell size can be used in combination with a collision limiter to decrease the computational time over a properly resolved DSMC calculation. DSMC simulations become computationally expensive as the density increases because of the large number of collisions that have to be computed and because the collision part of the DSMC code is the most expensive part of the DSMC method. Therefore, limiting the number of collisions in the virtually continuum regions can greatly decrease the computational time. The Titov and Levin<sup>14</sup> equilibrium DSMC (eDSMC) code utilizes a collision-limited approach to simulate high density flows, such as steady nozzle and supersonic channel flows. The eDSMC method is based on the DSMC method where the total number of collisions per cell per timestep is limited on average to two per molecule. For the flows that they studied, two collisions per molecule were sufficient to obtain a near equilibrium distribution in the cell. Their eDSMC method provided good agreement with high order Eulerian solvers for inviscid flows. For viscous flows, a hybrid eDSMC-DSMC method, where the eDSMC method is used to simulate the inviscid regions of the flow, provided good agreement with full DSMC simulations with a noticeable speed-up. Macrossan and Geng<sup>15</sup> also used a collision limited DSMC method in order to simulate steady rarefied flows with regions in thermal equilibrium. In their approach, they used two possible breakdown parameters to determine which cells are in thermal equilibrium. Once the different regions of the flow have been characterized, the non-equilibrium regions are computed using the DSMC method while the equilibrium regions are computed using the collision-limited version of the DSMC method. The collision limited computations were in good agreement with full DSMC simulations while using slightly less CPU time.

For fully transitional flows, another way to speed-up the simulations has been to use a parallel implementation of the DSMC solver. The DSMC method is well suited to parallelization because any molecule inside a given cell only interacts with the other molecules present in that cell at each timestep. To parallelize the DSMC code the computational domain is divided between the processors and each processor creates, moves and collides its own set of molecules. LeBeau's Distributed DSMC Analysis Code (DDAC)<sup>16</sup> is one example of a parallel implementation of the DSMC method. The DDAC solver is run on distributed memory systems using the Message Passing Interface (MPI) implementation. The full domain is divided between any given number of slave processors while one master processor oversees the I/O for the simulation. In order to optimize the efficiency of his method, LeBeau uses a dynamic domain decomposition where the decomposition of the domain between the processors is regularly updated for better load balancing. More recently, Wu and Tseng<sup>17</sup> used a very similar approach in their parallel implementation of the DSMC method. One major difference is in the repartitioning of the domain mainly due to the unstructured mesh used by Wu and Tseng.

The present DSMC code is being used to simulate the late stages of a comet impact on the Moon using the data computed by the continuum SOVA hydrocode for the near field of the impact event. The SOVA hydrocode<sup>18</sup> is used in the planetary science community to simulate impact phenomena including phase changes and large surface deformations but it is limited in its ability to model the far field gas dynamics. For that reason, at a fixed interface, the supersonic unsteady flow resulting from the impact is simulated with our DSMC code using the SOVA data at that interface as input. In this paper, we concentrate upon the unsteady far field gas dynamics computed via DSMC. A companion paper will emphasize the planetary science aspects of the hybrid results<sup>19</sup>. The objectives of this paper are to provide an overview of the DSMC code as well as to present some unique validation simulations that have been run. First, the specific characteristics of the three-dimensional serial DSMC code will be presented before detailing the parallel implementation. Then, the unsteady interface between the continuum solver and the DSMC code will be described in detail as well as some specific assumptions related to the simulations of an expansion into a vacuum. Results obtained for the unsteady expansion of a spherically symmetric gas cloud into a vacuum will then be compared to one-dimensional analytical results. Finally, three-dimensional validation simulations of the far field of a comet impact on the Moon will be compared to the SOVA hydrocode results in a region where both methods should produce valid results.

## II. Numerical method

### A. Three-Dimensional Spherical DSMC Code

The present DSMC code is an extension of the two-dimensional code used by Zhang *et al.*<sup>7, 20</sup> to simulate the sublimation atmosphere and volcano plumes on Jupiter's moon Io. The original code is designed for the simulation of atmospheric flow with such specific features as a gravity field, multiple species (including solid grains and condensates), internal energy exchange, radiation from the rotational and vibrational lines, discrete vibrational bands and a spherical coordinate system. In the two dimensional code, the location of a molecule is given by its radial distance from the center of the planet,  $\eta$  and its polar angle,  $\Theta$ . The main advantage of using spherical coordinates is that the surface of the planet is exactly represented by the lower boundary of the domain. The molecules are created as part of an initial atmosphere or are sublimated from the surface based on the surface temperature. They are then moved under the gravity field and can be lost due to escape or by falling back and sticking on the surface. During collisions, a variable hard sphere model is used to represent the interaction between the molecules and energy transfers to the rotational and/or vibrational modes are allowed during the collision event. A sequential steady multi-domain calculation can also be used in order to resolve the inner core of a supersonic plume both spatially and temporally (for very small radiative decay time scales).

This previous implementation could only study axisymmetric problems so the code has been modified to simulate full planetary flows and non axisymmetric plumes or expansions. The current implementation is now three-dimensional where the location of a molecule is given by its radial distance from the center of the planet,  $\eta$ , and its polar and azimuthal angles  $\Theta$  and  $\varphi$ , respectively. In the 2D version of the code, the boundary conditions applicable at the surface of the planet were a sticking boundary or specular or diffuse reflections. In the 3D code, a molecule can now stick to the surface of the planet with a mean residence time, determined by the surface temperature, before being released from the surface. This new boundary condition is required to simulate the late stages of a comet impact on the Moon. Indeed, after the impact, the few water molecules that have returned to the surface are expected to migrate on the surface due to the variations in the surface temperature. Finally, while the main species used for Io's simulations was  $\text{SO}_2$ , all the results presented here have been obtained for  $\text{H}_2\text{O}$ .

### B. Parallel Implementation

Non-axisymmetric unsteady expansion simulations are computationally expensive, so the three-dimensional DSMC code has been modified using the Message Passing Interface (MPI) implementation<sup>21</sup> in order to run on multi-processor systems. The full DSMC domain is divided between the processors and molecules are passed between processors. In the current implementation, a fixed domain decomposition is used so each processor computes the same region of the domain for the entire run. For the expansion simulations, the origin point of the expansion is assumed to be at the "North Pole" so a logical decomposition of the full domain is into smaller sub-domains in the azimuthal direction.

The actual speed-up obtained with the current parallel implementation of the code is highly dependent on two factors: the number of communications per timestep and the load balancing between the processors. The number of communications between processors has to be limited so that the overhead of a simulation remains small as the number of processors is increased. Currently the number of global communications has been limited to two per timestep. A first global communication sends across the number of molecules that a given processor will receive from each of the other processors, and then the data on the molecules are sent across in a single second communication. In order to do so, the molecules are sorted at the end of the move step so all the molecules going from a given processor to another given processor are grouped together. The decomposition of the domain is currently chosen by trial and error at the beginning of each simulation so the workload is fairly equally divided between processors. For oblique comet impacts, for instance, the flow heads mostly in the downrange direction so the processors upwind of the impact point are made to compute a larger domain than the downrange ones. Conversely, for vertical impacts, a uniform distribution of the domain between processors will provide nearly ideal load balancing.

### C. Uncoupled Unsteady Interface

In the most general case, the coupling between the continuum solver and the DSMC code in hybrid methods would be fully integrated so information could be transferred from either region to the other<sup>10</sup>. However, in the limiting case where the flow is appreciably supersonic at the interface between the continuum and rarefied regions, a

unidirectional coupling is sufficient because in supersonic flows, information cannot travel back upstream<sup>12</sup>. The present hybrid method uses a unidirectional version of the Roveda *et al.*<sup>10</sup> coupling from the continuum solver to the DSMC code.

In the case of a comet impact or an explosive expansion into a vacuum, the flow remains supersonic for most (if not all) times, so information does not travel back upstream. For that reason, the continuum solver can be run first and at a chosen interface the unsteady macroscopic data (density, pressure, temperature, etc.) can be saved (Figure 4 – Step 1). These data are later used as input to the DSMC simulations. For our purpose, we chose cells on a “connection hemisphere” at a constant distance from the point of origin of the expansion. For the comet simulations, the radius of the “connection hemisphere” has to be large enough so that densities and pressures in the selected cells are within a range that is acceptable for the molecular code. Moreover, the interface cannot be too far from the impact point since the accuracy (and cost) of the hydrocode computation of the impact event must also be taken into account. A reasonable radius for the “connection hemisphere” for a “standard” impact was found to be about 20 km. The interface itself is made-up of individual cells so the geometry of the interface also has to be input in the DSMC simulations in addition to the macroscopic data (Figure 4 – Step 2). In the present example, the interface cells in the continuum code are Cartesian so they will not precisely overlap with the spherical DSMC cells (Figure 4). For that reason, molecules are created inside the Cartesian interface cells using an acceptance-rejection method and, after a DSMC move step, the molecules that did not drift out of the interface cells to enter the DSMC domain are deleted (Figure 4 – Steps 3 and 4). That is, an equilibrium distribution of molecules is created in the Cartesian boundary cells and allowed to drift into the spherical DSMC grid. For parallel simulations, the interface data are split up between processors and a processor will only consider the interface cells that have their cell centers within its boundaries. If some of the newly created molecules are outside of the processor boundaries these molecules are transferred to the appropriate processor at the end of the creation step. The interface between the codes is unsteady and the DSMC molecules are created at each timestep based on the continuum solver data at that time. If the continuum solver timestep is larger than the DSMC timestep, which is usually the case, the data from that timestep are repeated until the DSMC code catches up to the continuum solver’s time.

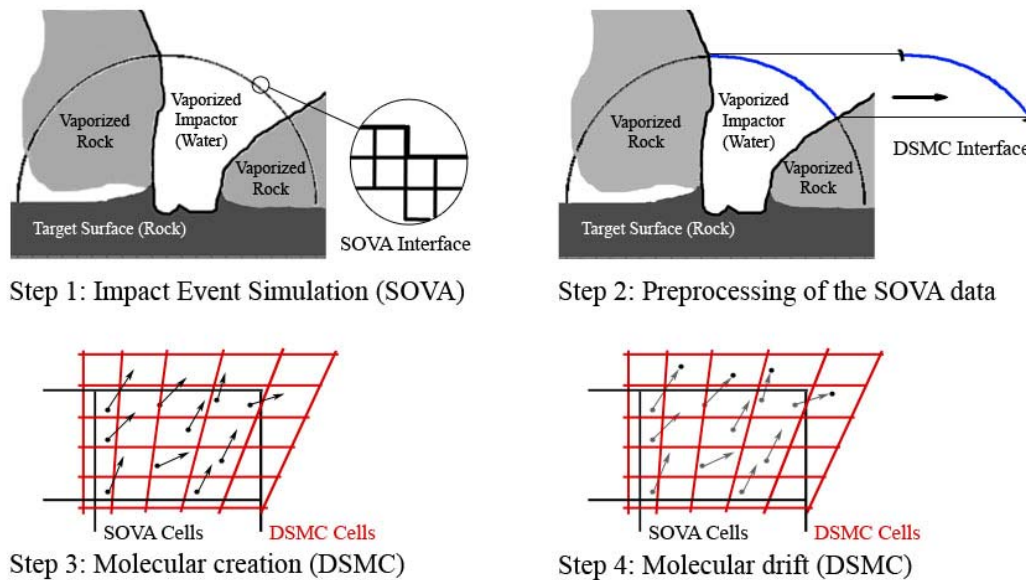


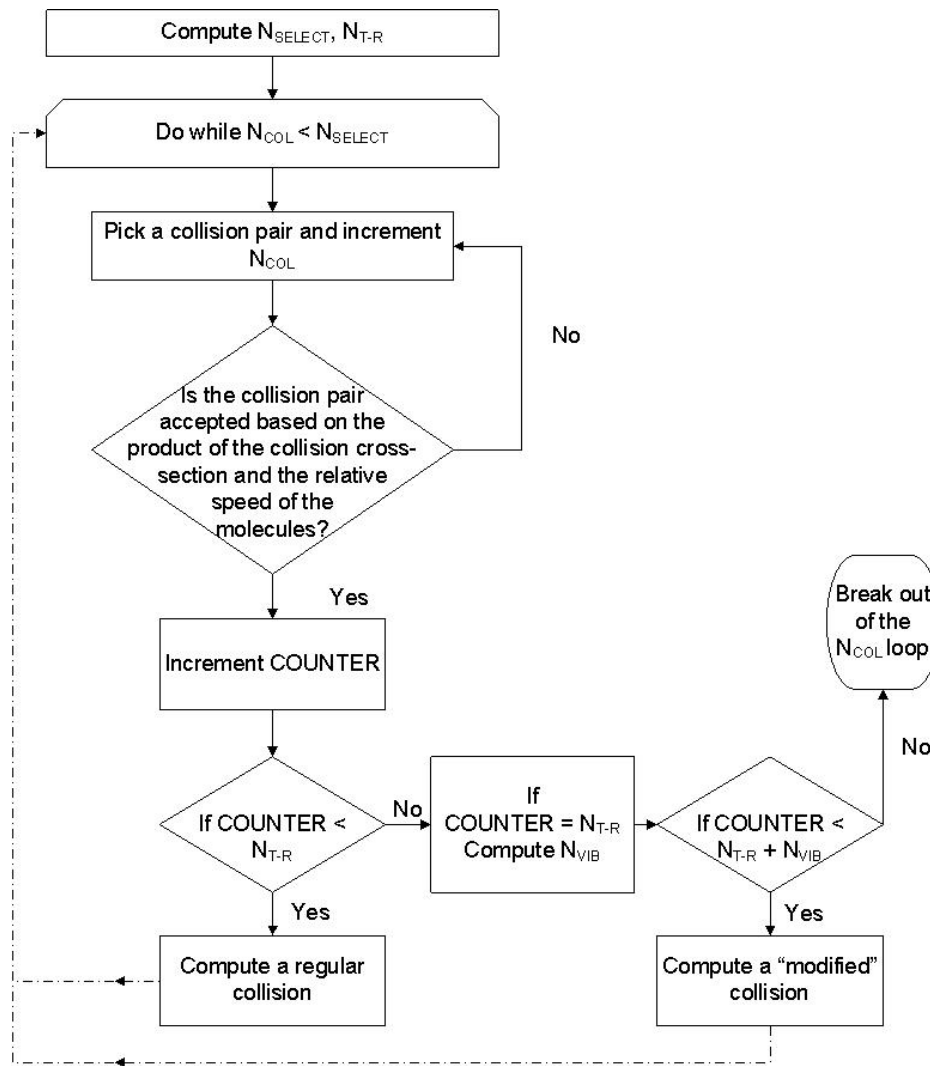
**Figure 1. Schematic of the hybrid SOVA-DSMC method used to simulate a comet impact on the Moon.**

#### D. Collision Limiter

Due to the computational cost of the simulation of the impact event using a hydrocode, the interface between the SOVA hydrocode and the DSMC code is in the near continuum region of the flow. In these high density regions of the flow, the mean free path can be on the order of microns. However, the DSMC domain for the comet impact simulations is to be tens of kilometers in each direction and, therefore at best, even for parallel computations, the cell size can only be in the meter range. In the DSMC method, the preferred cell size is of the order of the mean free path and the timestep should be smaller than the average time between collisions. Therefore, for the proposed simulations, it will not be feasible to satisfy the usual constraints on cell size and timestep to obtain an accurate solution close to the impact point. However, we are mostly interested in the far field deposition of the water so an approximate approach to modeling the dense transitional regions was deemed acceptable. Hence, we choose to use an under-resolved collision-limited DSMC solution with large cells and timestep in the near field as a transition to a resolved far field DSMC solution. The overall effect of such an approximation is to misrepresent the transport coefficients (e.g., the effective viscosity is too large). Fortunately, the gradients of the flow are expected to be small, with length scales greater than the cell size, in the under-resolved regions of the flow and hence errors in the transport coefficients should have a minimal effect on the flow. In addition, the inviscid SOVA code (aside from numerical viscosity) produces gradients only across its  $O(10m)$  sized cells. Since the flow is rapidly expanding, these lateral and radial gradients are dissipating and we expect that even our crude collision limited DSMC can track them.

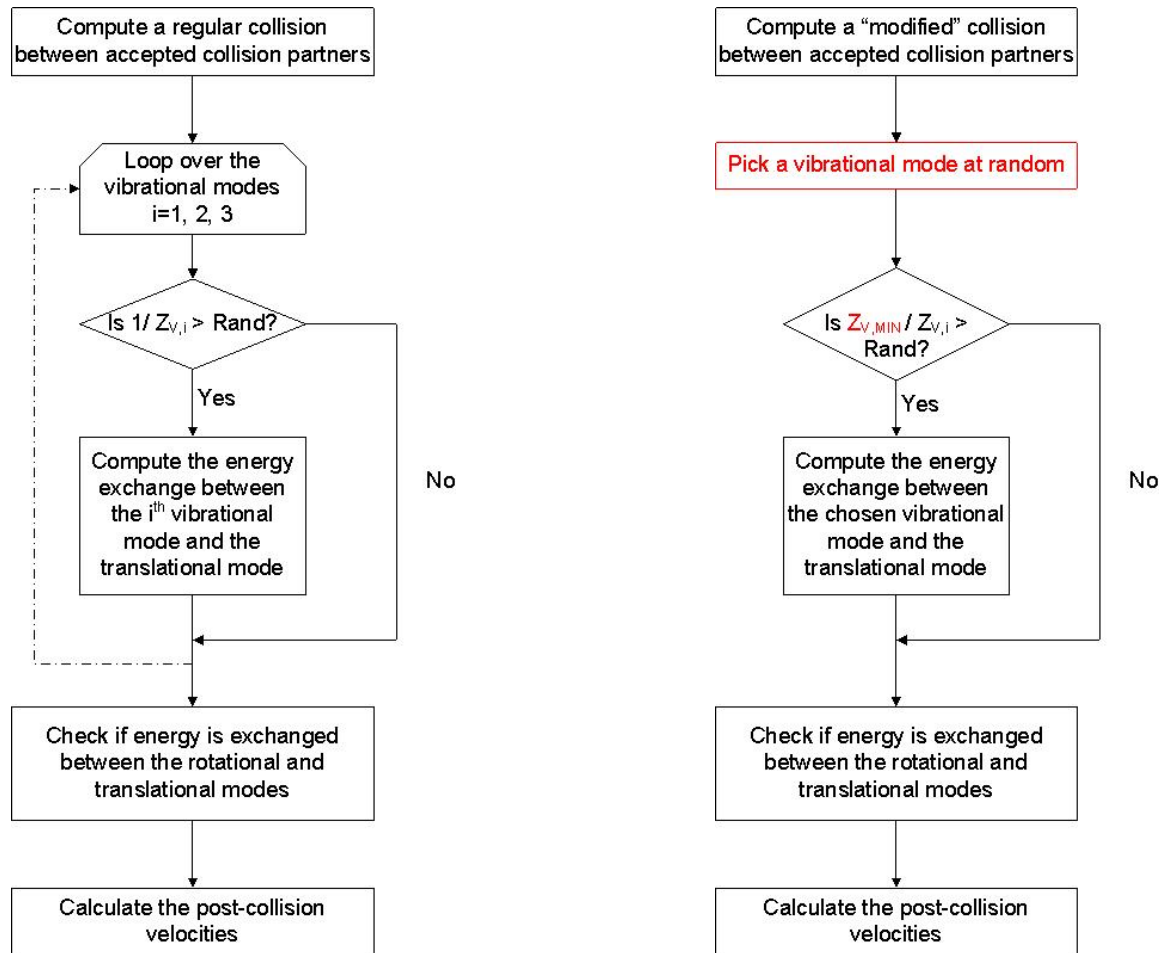
Similar to the eDSMC method<sup>14</sup>, a collision limiter is used in the present simulations to speed-up the code. The algorithm for the collision subroutine in the case when the collision limiter is utilized is presented in Figure 2. At the beginning of the collision subroutine, the number of pairs of molecules that should be selected per timestep per cell ( $N_{SELECT}$ ) is calculated using the No Time Counter (NTC) method<sup>1</sup>. In addition, the collision limit  $N_{T-R}$  is also computed. The code then starts to loop over the number of collisions. A pair of molecules is picked at random from the cell and the pair is accepted for collision based on the value of the product between its collision cross-section and the relative speed of the molecules. If the pair is accepted, the collision is computed. If the number of accepted collisions is lower than  $N_{T-R}$ , a regular collision is computed.  $N_{T-R}$  is chosen such that the translational and rotational energy modes of a molecule equilibrate with those of other molecules in a cell. In the current simulations, the rotational relaxation collision number is fixed at 2.5 and  $N_{T-R}$  is chosen to be 5 times the number of molecules in the cell.

The Titov and Levin<sup>14</sup> and Macrossan and Geng<sup>15</sup> collision limiters have been used to simulate flows of monatomic and diatomic gases. In the present simulations, we are interested in the expansion flow of water vapor after a comet impact. Water is a triatomic molecule with three vibrational modes: the  $v_1$  and  $v_3$  stretching modes and the  $v_2$  bending mode. If a cell is in equilibrium each vibrational mode of the water molecules needs to also be equilibrated. However, the vibrational relaxation collision number for each mode is much larger than the rotational relaxation collision number and hundreds of collisions have to be computed before a vibrational mode will exchange energy with the other energy modes. For that reason, after only 5 collisions on average per molecule the vibrational modes will not be equilibrated so  $N_{VIB}$  additional “modified” collisions are computed. During a “modified” collision, exchange of energy between the vibrational and the translational mode is forced to be more probable so each one of these collisions represents hundreds of regular collisions and enables a faster equilibration of the vibrational energy modes of a molecule. Thus after the  $N_{T-R}$  regular collisions and the additional  $N_{VIB}$  “modified” collisions the cell will be in equilibrium.



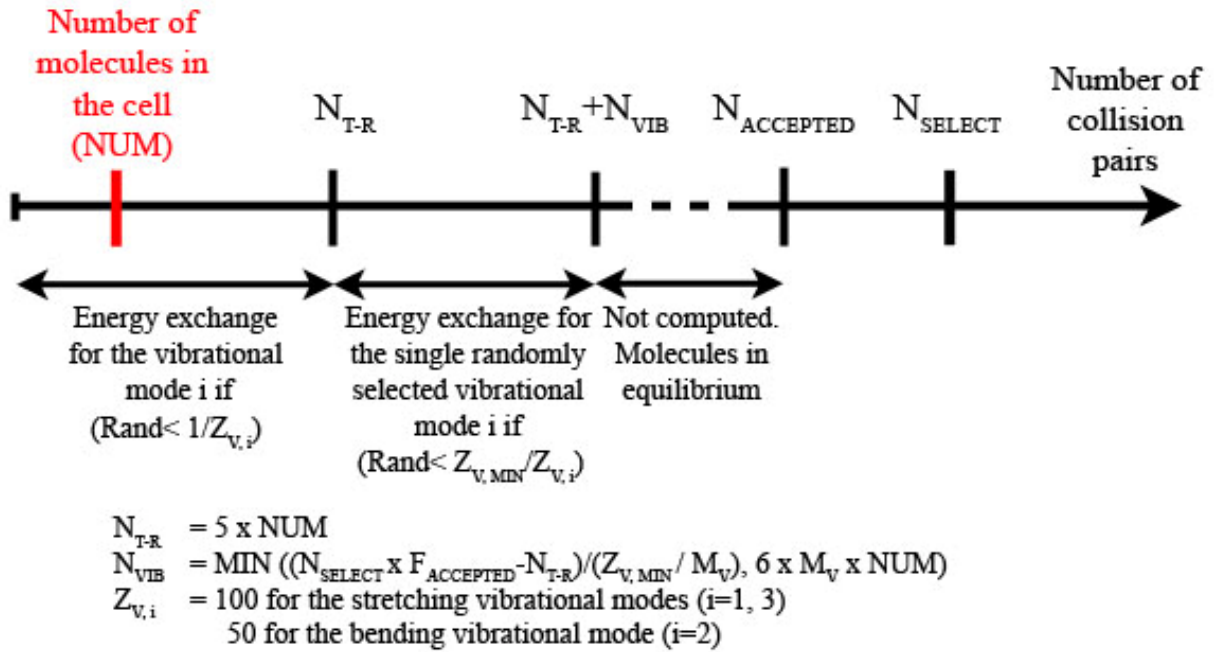
**Figure 2. Flowchart of the collision subroutine when the collision limiter is turned on.**

Figure 3 details the differences between regular and “modified” collisions. During a regular collision the probability of energy exchange between a vibrational mode and the translational mode is based on the vibrational relaxation collision number for that given vibrational mode using the Larsen-Borgnakke method<sup>1</sup>. In a “modified” collision the probability of a given vibrational energy exchange is increased by the value of the minimum vibrational collision number for the entire simulation. In the current simulations, the vibrational collision numbers for the water molecules have been fixed at 50 for the  $\nu_2$  bending mode and at 100 for the  $\nu_1$  and  $\nu_3$  stretching modes. The minimum vibrational collision number is relaxed at every timestep to a value that will be near 50 in the present simulations and thus if selected the  $\nu_2$  mode will almost always exchange energy with the translational mode in a “modified” collision. From some preliminary simulations, where each “modified” collision had possible energy exchange with all three modes we noticed that the order in which the modes were considered mattered, unlike what happens if only standard DSMC collisions are used<sup>1</sup>. For that reason, a “modified” collision now considers only one vibrational mode picked at random for possible energy exchange instead of considering all three modes.



**Figure 3. Flowchart for a regular (left) and "modified" (right) collision.**

Figure 4 is a schematic representation of the scale of each collision number variable in a region of flow where the timestep is much larger than the mean collision time and therefore  $N_{\text{SELECT}} \gg \text{NUM}$  and, in general,  $N_{\text{SELECT}} > N_{\text{ACCEPTED}}$ . In the current simulations,  $N_{\text{T-R}}$  is chosen to be 5 times the number of molecules in the cell since this will allow equilibration of the translational and rotational modes. While selecting potential collision partners up to  $N_{\text{T-R}}$  accepted collisions, the number of selections needed is counted. This allows for the fraction of accepted collisions,  $F_{\text{ACCEPTED}}$ , to be estimated by the ratio of needed selections over  $N_{\text{T-R}}$ . Once the translational and rotational modes are equilibrated,  $N_{\text{VIB}}$  additional "modified" collisions, each of which represent  $Z_{\text{V,MIN}}$  accepted collisions for each mode, are performed to transfer vibrational energy. The number of "modified" collisions,  $N_{\text{VIB}}$ , to perform is computed by dividing the product of the number of vibrational modes ( $M_{\text{V}}$ ) and the estimated number of accepted collisions remaining after the  $N_{\text{T-R}}$  collisions are performed ( $F_{\text{ACCEPTED}} \times N_{\text{SELECT}} - N_{\text{T-R}}$ ) by the minimum average number of collisions for vibrational energy transfer ( $Z_{\text{V,MIN}}$ ) (Figure 4). The previous equation is an approximation of what  $N_{\text{VIB}}$  should exactly be because in theory  $N_{\text{VIB}} = (M_{\text{V}} * (N_{\text{ACCEPTED}} - N_{\text{T-R}}) / Z_{\text{V,MIN}})$ . Unfortunately, using the NTC method  $N_{\text{ACCEPTED}}$  is only known once all the collisions have been computed so in the present simulations it has been approximated by  $F_{\text{ACCEPTED}} \times N_{\text{SELECT}}$ . In addition,  $N_{\text{VIB}}$  is capped at 6 per vibrational mode ( $M_{\text{V}}$ ) per molecule since after that many "modified" collisions the vibrational modes will be equilibrated. All additional collisions beyond  $N_{\text{T-R}} + N_{\text{VIB}}$  are not performed because the gas in that cell is already in equilibrium.



**Figure 4. Scaling of all the variables considered in the collision subroutine for an under-resolved high density flow. The total number of accepted collisions is limited to a few per molecule. Equilibration of the translational modes and rotational modes is achieved thru  $N_{T-R}$  regular collisions. Energy exchange with the vibrational modes is then computed by adding a few  $N_{VIB}$  additional “modified” collisions where the probability of translational-vibrational energy exchange is increased.**

As the flow expands away from the point of origin, the density of the flow drops rapidly and the number of selected pairs ( $N_{SELECT}$ ) calculated using the NTC method will also start to decrease. At some point,  $N_{SELECT}$  will be small enough (on the order of a few hundred) such that the vibrational modes should start to freeze out. In that case, in our collision-limited code,  $N_{VIB}$  is set to  $M_v * (F_{ACCEPTED} \times N_{SELECT} - N_{T-R}) / Z_{v,MIN}$  which enables only partial equilibration of the vibrational modes and freezing of the vibrational temperatures should be observed. Even later in the expansion,  $N_{SELECT}$  will become smaller than  $N_{T-R}$  and in that case the simulation is no longer collision-limited and will revert to a classic DSMC computation.

### III. Results and discussions

#### A. 1D Unsteady Expansion into a Vacuum

The problem of the expansion of a gas cloud into a vacuum has been studied since the late fifties using several simplifying assumptions. Sedov<sup>22</sup> was the first to study several similarity problems such as explosions from a point source or spherical detonations. However, these problems involved the presence of a background gas and so a year later, Stanyukovich<sup>23</sup> provided one of the first solutions for the problem of the expansion of a gas cloud into a vacuum for a gas initially occupying a finite volume of radius  $R_0$ . A few years later, Zel’dovich and Raizer<sup>24</sup> and even more recently Tzuk *et al.*<sup>25</sup> revisited the results obtained for the expansion of a gas into a vacuum.

Expansion flows into a vacuum can be related to several engineering problems, such as nozzle plumes used in spacecraft applications and desorption or laser ablation from a surface. In many cases, the DSMC method was coupled to another solver in order to resolve such flows. Kannenberg and Boyd<sup>3</sup> simulated 3D rarefied plume impingement flows using the DSMC method and more recently, VanGilder *et al.*<sup>26</sup> used a hybrid CFD-DSMC

method to study the 3D unsteady plumes from a high altitude missile. The DSMC method has also been used as a tool to study some of the physics of rarefied expansion flows such as freezing of the rotational and vibrational temperatures<sup>27,28</sup>. But these problems were assumed to be quasi-steady in which time-averaging could be used in the DSMC portion. Bykov *et al.*<sup>29</sup>, however, used a unidirectional hybrid approach to study the unsteady expansion of vaporized metals into a vacuum induced by the pulsed laser ablation of a target surface. Their model first solves for the laser radiation absorption by the surface and calculates the surface induced heating and vaporization rates. They then studied the unsteady gas dynamics of the vaporization products using the DSMC method.

The first benchmark test for our approach has been to compare our DSMC results with an analytic solution for the expansion of a gas cloud into a vacuum. The analytic solution provides the required boundary condition (in place of SOVA) at the interface with the DSMC code and the DSMC results are then compared to the analytic solution downstream of the interface. The scale of the expansion has been chosen to be representative of the scales of a comet impact in order to test our approach and, in particular, our collision-limiting scheme.

### 1. Analytic solution

The analytic solutions used in the present tests have been obtained using the following assumptions based on Tzuk *et al.*<sup>25</sup>. An ideal gas cloud is initially confined inside a sphere of radius  $R_0$ . At  $t=0$ , the “separation” from the vacuum is removed and the outer shells of the sphere begin to expand into the vacuum. The flow during the expansion is assumed to be isentropic and the initial density and pressure distributions inside the sphere have a specific form that allows for an analytic solution to be found for the late times of the expansion<sup>25</sup>. While the early time results are dependent on  $R_0$ , this dependence disappears as  $t \rightarrow \infty$ . The expansion of this initial sphere of gas into a vacuum is governed by the equations (1) to (4) found in Tzuk *et al.*<sup>25</sup>. As  $t \rightarrow \infty$ , a simple solution is found for the density and temperature distributions as

$$\begin{aligned} \rho &= \frac{AM}{u_{\max}^3 t^3} \left( 1 - \left( \frac{r}{u_{\max} t} \right)^2 \right)^B \\ T &= T_0 \left( \frac{R_0}{u_{\max} t} \right)^{3(\gamma-1)} \left[ 1 - \left( \frac{r}{u_{\max} t} \right)^2 \right] \end{aligned} \quad (1)$$

$$u_{\max}^2 = u_{\infty}^2 \frac{5+2B}{3}, u_{\infty} = \sqrt{\frac{2Q}{M}} \text{ and } B = \frac{1}{\gamma-1}$$

with

$$\begin{aligned} A &= \frac{\Gamma\left(\frac{5}{2} + B\right)}{2\pi\Gamma\left(\frac{3}{2}\right)\Gamma(B+1)} \\ T_0 &= \frac{\left(\frac{Q}{M}\right)(\gamma-1)}{R} \end{aligned} \quad (2)$$

and where  $\rho$  is the density,  $t$  is the time,  $u$  is the radial velocity component,  $r$  is the distance from the center of the cloud,  $\gamma$  is the ratio of specific heats,  $T$  is the temperature,  $R$  is the specific gas constant,  $M$  is the mass of the gas,  $Q$  is the total energy of the gas,  $\Gamma$  is the gamma function and  $u_{\max}$  is the velocity of the outer layers of the cloud.

### 2. Numerical results

The initial conditions used in the present simulations have been chosen so the flow time and velocity scales are comparable to those for a comet impact on the Moon. Using these properly chosen initial conditions for a gas cloud made out of water vapor, the outer shell of the cloud travels at 20 km/s. The results presented below are at a time well after the beginning of the expansion and the values for the temperature, velocity and density are calculated as a function of time at the interface using the analytic solution presented in Section (3.1.1.). With the prescribed boundary conditions, 2 s after the beginning of the expansion, the Knudsen number based on the density gradient at 20 km is tiny, only about  $6 \times 10^{-9}$  ( $Kn_{\text{GLL}}$  in Roveda *et al.*<sup>10</sup>). Currently the interface is a hemisphere of radius  $r = 20$

km made of small Cartesian cells of a maximum cell size of 150 m. The geometry of the interface is exactly the same as the one used in the impact simulation as provided by the SOVA hydrocode simulations (Figure 5). The analytic solution is one-dimensional but is calculated at every SOVA interface cell based on the distance of the cell center away from the point of origin. The present simulations have been run with the three-dimensional serial version of our DSMC code. However, in order to be compared to the one-dimensional analytic solution, the DSMC results presented in Figure 6 and Figure 7 have been sampled in radial bins.

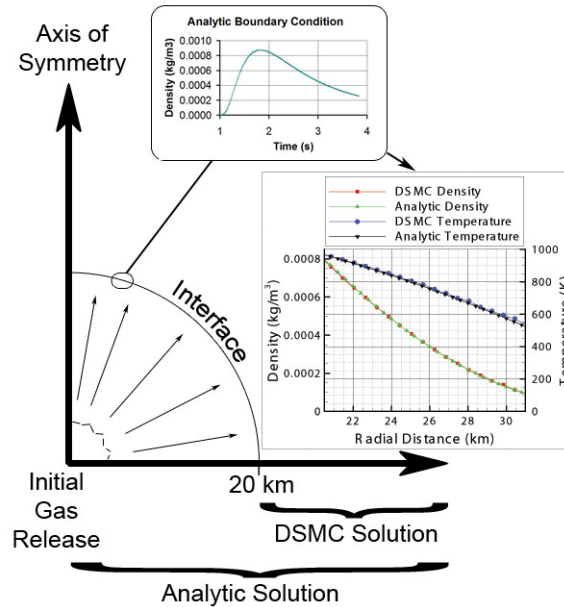


**Figure 5. Schematic of the hybrid solver used to simulate the one-dimensional expansion flow into a vacuum.**

The DSMC domain is a 30 km by 30 km by 0.5 degree “piece of pie” using 180000 cells and containing about 10 million molecules and with a timestep of 0.01s. In order to obtain a more accurate solution a free cell approach has been added in the collision part of the DSMC code<sup>10</sup>. Molecules chosen as collision partners will only be accepted if they are inside a prescribed region around the initial molecule. Depending on the size of the prescribed region, it is possible that no partner will be present. In that case, the size of the region is increased incrementally until a partner is found. The sampled DSMC results obtained 2 s after the beginning of the expansion are compared to the analytic solution in Figure 6 and Figure 7. Good agreement has been obtained for the density and velocity profiles (Figure 6) where the DSMC results nearly overlap the analytic solution.

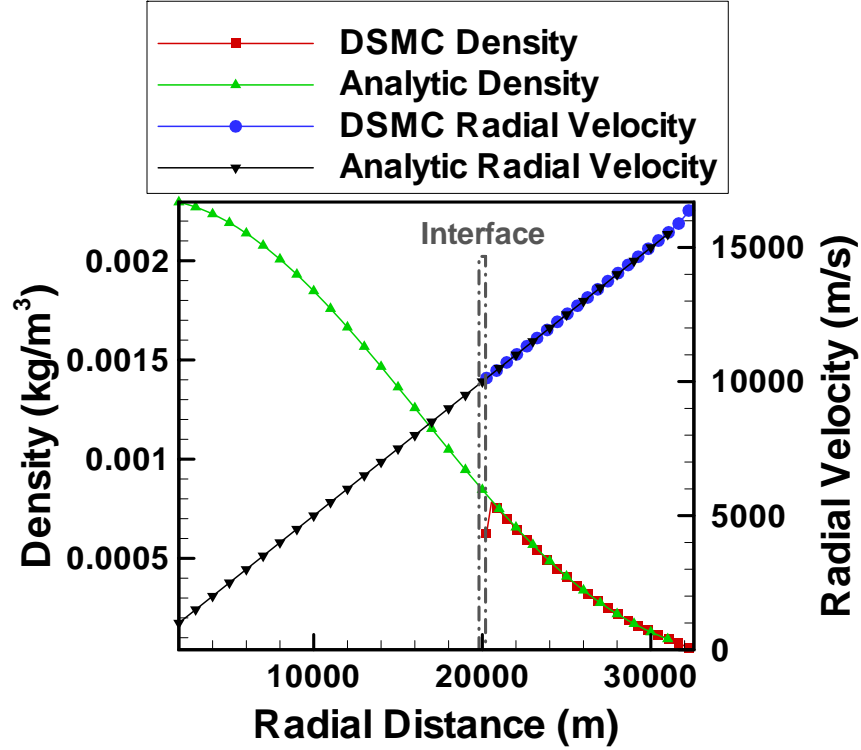


**Figure 6.** DSMC and analytic density profiles and radial velocity versus radial distance from the point of origin of the expansion.

In Figure 7, the total, translational and rotational temperatures are also in very good agreement with the analytic solution. The vibrational temperatures have also been plotted in Figure 7 using the following equation for the vibrational temperature of mode  $v_i$ :

$$T_{V,i} = \frac{\theta_i}{\log\left(1 + \frac{R\theta_i}{e_{V,i}}\right)} \quad (3)$$

where  $\theta_i$  is the characteristic temperature of the mode  $v_i$ ,  $R$  is the specific gas constant and  $e_{V,i} = \sum_{k=1}^{\infty} R \times k \times \frac{N_k}{N} \theta_i$

with  $N$  being the total number of molecules and  $N_k$  the number of molecules in the  $k^{\text{th}}$  excited level.

In Figure 7a, the average vibrational temperatures for each bin have been obtained by *averaging the vibrational temperatures* in each DSMC cell. As a result, the vibrational temperatures for the stretching modes  $v_1$  and  $v_3$  are too low and are noticeably smaller than the vibrational temperature for the bending mode  $v_2$  (Figure 7a). The discrepancies between the three vibrational temperatures are due to the fact that the vibrational stretching modes  $v_1$  and  $v_3$  have very similar characteristic temperatures,  $\theta_1=5261\text{K}$  and  $\theta_3=5404\text{K}$  respectively, that are much larger than the characteristic temperature for the bending mode  $v_2$ ,  $\theta_2=2438\text{K}$ . These characteristic temperatures are much larger than the analytic temperature of several hundred Kelvins so a large number of molecules per cell is required to obtain an accurate solution in a single cell for the vibrational temperatures. In the current simulation, more than 100 (instantaneous) molecules are present, on average, in each cell up to 26 km away from the point of origin which is sufficient to represent the translational, rotational and mode  $v_2$  vibrational temperatures accurately. Further away,

once the number of molecules falls below that threshold, the statistics are no longer sufficient even for the vibrational mode  $v_2$  and the agreement with the analytic solution worsens. The number of cells without even one vibrationally excited molecule (ie. with a vibrational temperature of zero) increases and thus the averaged vibrational temperatures are too low. One way to obtain better statistics is to average the DSMC molecular data into larger cells. In Figure 7b, we calculate the vibrational temperatures in a radial bin using the vibrational populations inside all the DSMC cells present in the entire bin. This can be seen as a spatial averaging that can be used in this case more readily than a standard ensemble averaging. The results obtained using population-averaging provide a much improved agreement between the vibrational temperatures and the analytic temperature.

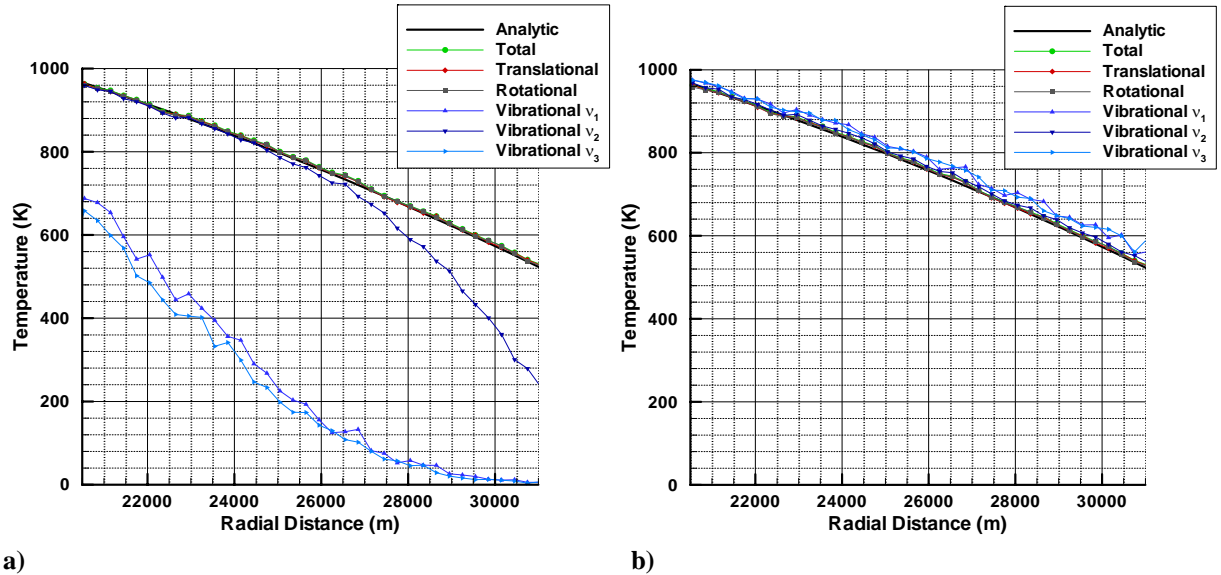


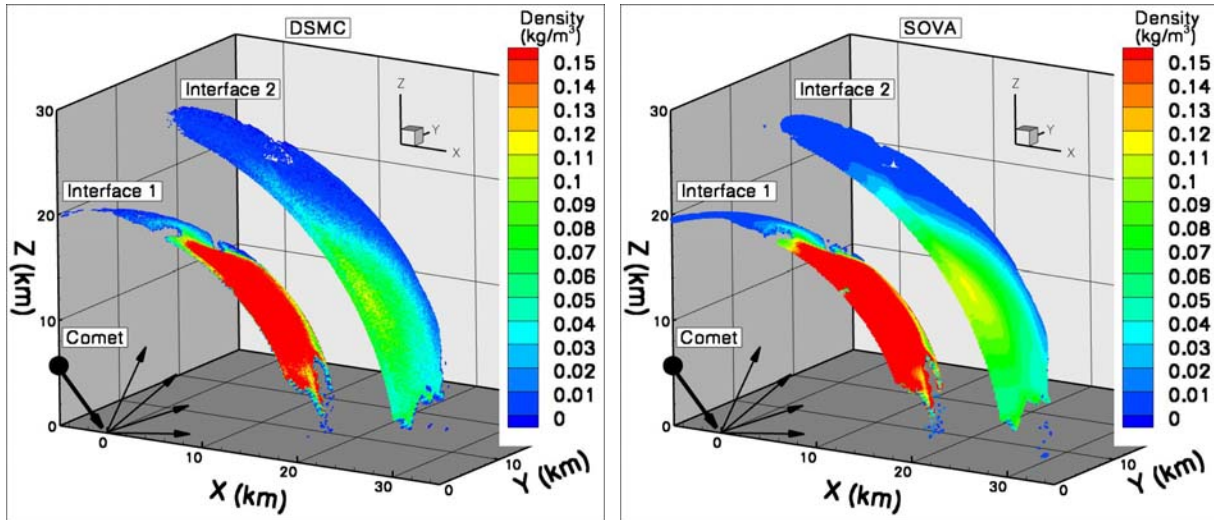
**Figure 7. DSMC and analytic temperature profiles versus radial distance from the point of origin of the expansion using (a) a sampling of the vibrational temperatures in each radial bin and (b) a sampling of the populations in each vibrational state.**

### 3. Late Stages of a Comet Impact

The method of choice to simulate a crater-forming impact is by using a hydrodynamic code such as CTH<sup>30, 31</sup> or SOVA<sup>16</sup>. The SOVA hydrocode simulates the first few seconds of a comet impact event using a two-step Eulerian scheme to solve the equations of hydrodynamic flow in finite difference form. The simulation starts with the impactor near the surface of the target with a given velocity vector. The run then proceeds by calculating the pressure and temperature changes in both objects, first, as an irreversible shock compression and then an isentropic decompression pass through them. The pressure and temperature variations induce phase change in the materials and the degree of melting and vaporization of each material is calculated using tabulated equations of state for the given materials. The time evolution of each material is followed by Lagrangian tracers initially distributed in both the target and the impactor. The amount of material vaporized as well as its temperature, density and velocity are all dependent on the size, velocity and angle of impact of the comet and the initial composition of both the comet and the target.

The present computations simulate the impact of a comet on the surface of the Moon. The impactor is a sphere of packed snow 1 km in radius that hits the surface at a 45° angle with a velocity of 30 km/s. The SOVA simulations are run for 12 s after impact and unsteady data are saved at two concentric hemispheres, interfaces {1} and {2}, which are 20 km and 30 km in radius, respectively. In the DSMC simulations, we neglect the rock inside the SOVA cells at the interfaces and only use the water data. Because the boundary between the water and rock is not well handled by the continuum approach used in the hydrocode, and as only a minor portion of the water is near the boundary with the rock, the water data in cells containing both rock and water vapor is currently ignored. In addition, the water is assumed to be purely in the vapor phase at the interface and to remain so within the DSMC domain. The DSMC simulations have been run on the Texas Advanced Computing Center (TACC) supercomputer Lonestar using 32 processors. The entire domain is divided into 18.4 million cells and a peak of about 5 million

instantaneous molecules per processor was used. The present validation runs compare macroscopic data at both interfaces {1} and {2} obtained from the full SOVA simulations and from the hybrid SOVA-DSMC simulations. Figure 8 and Figure 9 show contours of density and temperature at the interfaces {1} and {2} as seen from the plane of symmetry of the impact. The comet comes at a 45° angle from the left and the plume expands away mostly in the downrange direction to the right. The density contours are shown in Figure 8. There is good quantitative agreement between the codes at both the creation interface (interface {1}) as well as the downstream interface (interface {2}) and the overall shape of the expansion plume is similar.

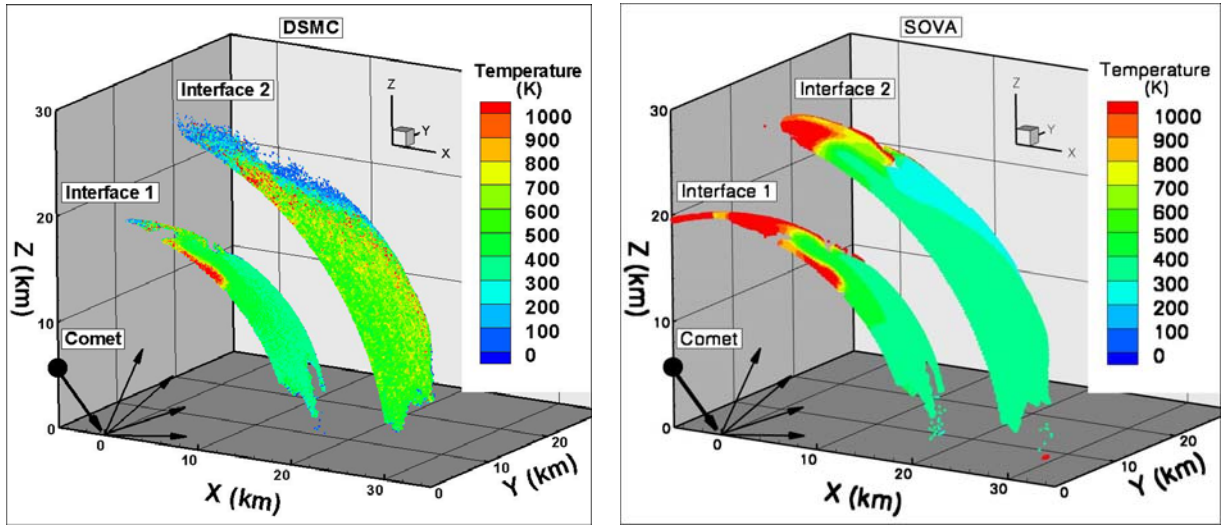


a)

b)

**Figure 8. Density contours at interfaces {1} and {2}, 1s after the impact, from the (a) DSMC and (b) SOVA simulations.**

The temperature contours are presented in Figure 9. It can be seen that the DSMC results (Figure 9a) do not perfectly match the SOVA solution (Figure 9b). In order to obtain a smoother solution, ensemble averaging as well as temporal averaging have been used to plot the DSMC contours presented in Figure 9a. In the present simulations the DSMC timestep is smaller than the SOVA timestep so even if the simulation is unsteady, a temporal averaging of the DSMC solution over a SOVA timestep has been utilized. Even with these two statistical averaging approaches, the DSMC solution does not match the SOVA solution well in the low density regions. First, at interface {1}, the high temperature region right above the impact point is not well captured in the DSMC simulations. This region has only a few representative molecules per cell and an accurate solution cannot be expected. At interface {2}, the low density regions are again hard to resolve but in addition, the temperature from the DSMC simulation is very noisy and appears to be a little too high even in the high density region of the flow. The focus of the project is to follow the water until it is destroyed or falls back on the lunar surface. Hence, the good agreement between the DSMC and SOVA densities and velocities and modest agreement on temperature should provide us with accurate enough results for the later circum-lunar part of the simulations.



a)

b)

**Figure 9. Temperature contours at interfaces {1} and {2}, 1 s after the impact, from the (a) DSMC and (b) SOVA simulations. Note that the cells that have two molecules on average or less in the DSMC simulation have been blanked out in the left figure.**

Figure 10 is a plot of the density contours in the plane of symmetry of the previous impact 1s after impact. The contours below the red interface and the black and grey lines above it are from the SOVA simulation of the impact event. The grey contours represent water and the green ones represent the rock with the darker colors representing the denser regions of the flow. The color contours above the interface, with the associated legend, are from the DSMC simulation using the SOVA data at the interface as input. The DSMC data matches well some of the features of the SOVA plume above the interface. First, the overall shape of the plume is preserved as the DSMC contours fill in well the region of the plume where water was present in the SOVA simulation. Even the region filled with rock inside the water plume (elongated area lined by the black line within the water plume) can be observed as an empty area in the DSMC contours. However, one should note that as the flow expands, such regions will be slowly filled by water diffusing in from the surrounding regions because the rock is not computed in the DSMC simulation. Finally, the dense region of the water plume represented by the red contours in the DSMC simulation matches well the higher density region from the SOVA simulation bordered by the grey line above the interface.

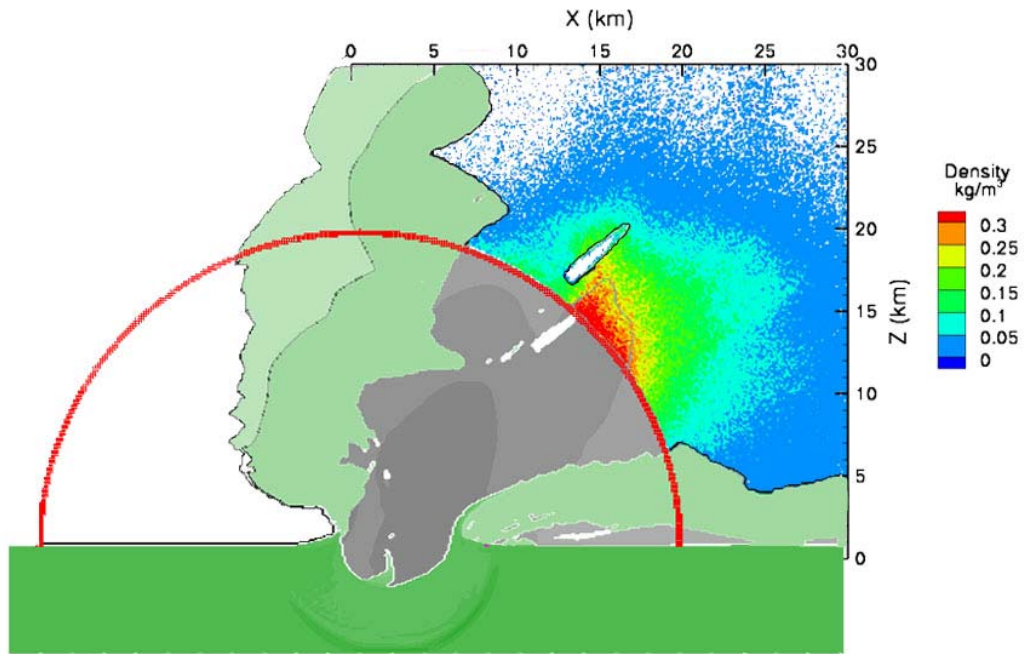


**Figure 10.** Density contours 1 s after the impact in the plane of symmetry of the impact. The green and grey contours are from the SOVA calculations and represent the rock and water densities, respectively. The color contours above the red interface represent the DSMC water density contours with the attached legend.

#### IV. Conclusions

Results from a hybrid simulation using a continuum solver and the DSMC method have been presented for a 1D unsteady expansion of a gas cloud into a vacuum and for the far field of a 3D expansion plume from a comet impact. The DSMC results have been successfully compared to the analytic solution for the 1D expansion and have provided some encouraging results for the late stages of the comet impact. The density contours and the overall shape of the plume compared favorably to the SOVA hydrocode results downstream of the creation interface, however the temperature contours were not perfectly matched.

#### Acknowledgements

This work is sponsored by the NASA Planetary Atmospheres program, under grant NNG04GQ66G. The authors also would like to acknowledge the Texas Advanced Computing Center (TACC) at The University of Texas at Austin for providing substantial computing resources.

#### References

<sup>1</sup>Bird, G. A., "Molecular Gas Dynamics and the Direct Simulation of Gas Flows," *Oxford University Press*, New York, pp. 218-256, 1994.

- <sup>2</sup>Nanbu, K., "Theoretical basis on the direct Monte Carlo method," *Rarefied Gas Dynamics*, edited by V. Boffi, C. Cercignani, Vol. 1, Teubner, Stuttgart, 1986.
- <sup>3</sup>Kannenbergh, K. C. and Boyd, I. D., "Three Dimensional Monte Carlo Simulations of Plume Impingement," *Journal of Thermophysics and Heat Transfer*, Vol. 13, No. 2, pp. 226-235, 1999.
- <sup>4</sup>Ngalande, C., Lilly, T., Killingsworth, M., Gimelshein, S., and Ketsdever, A., "Nozzle plume impingement on spacecraft surfaces: Effects of surface roughness," *Journal of Spacecraft and Rockets*, Vol. 43, No. 5, pp. 1013-1018, 2006.
- <sup>5</sup>Moss, J. N., Boyles, K. A. and Greene, F. A., "Orion aerodynamics for hypersonic free molecular to continuum conditions," *14<sup>th</sup> AIAA/AHI International Space Planes and Hypersonic Systems and Technologies Conference*, Canberra, Australia, 2006.
- <sup>6</sup>Austin, J. V., and Goldstein D. B., "Rarefied gas model of Io's sublimation driven atmosphere," *Icarus*, Vol. 148, pp. 370-383, Dec. 2000.
- <sup>7</sup>Zhang, J., Goldstein D. B., Varghese P. L., Trafton L. M., Miki K., and Moore C., "Numerical modeling of ionian volcanic plumes with entrained particulates," *Icarus*, Vol. 172, p. 479-502, Dec. 2004.
- <sup>8</sup>Moore, C.H., Goldstein, D. B., Varghese, P. L., Trafton, L. M., Stewart, B., "1-D DSMC Simulation of Io's Atmospheric Collapse and Reformation During and After Eclipse," *submitted for publication to Icarus*.
- <sup>9</sup>Walker, A.C., Gratiy, S.L., Levin, D.A., Goldstein, D.B., Varghese, P.L., Trafton, L.M., Moore, C.H., and Stewart, B., "Modeling Io's Sublimation-Driven Atmosphere: Gas Dynamics and Radiation Emission," *Rarefied Gas Dynamics: 26<sup>th</sup> International Symposium*, 2009.
- <sup>10</sup>Roveda, R., Goldstein, D. B., and Varghese, P. L., "Hybrid Euler/direct simulation Monte Carlo calculation of unsteady slit flow," *Journal of Spacecraft and Rockets*, Vol. 37, pp. 753-760, 2000.
- <sup>11</sup>Vashchenkov, P.V., Kudryavtsev, A.N., Khotyanovsky, D.V., and Ivanov, M.S., "DSMC and Navier-Stokes Study of Backflow for Nozzle Plumes Expanding into Vacuum," *Rarefied Gas Dynamics: 24<sup>th</sup> International Symposium*, pp. 355-360, 2005.
- <sup>12</sup>Papp, J.L., Wilmoth, R.G., Chartrand, C.C., and Dash, S.M., "Simulation of High-Altitude Plume Flow Fields Using a Hybrid Continuum CFD/DSMC Approach," *42nd AIAA/ASME/SAE/ASEE Joint Propulsion Conference and Exhibit*, Sacramento, 2006.
- <sup>13</sup>Schwartzentruber, T. E., Scalabrin, L. C. and Boyd, I. D., "A modular particle-continuum numerical method for hypersonic non-equilibrium gas flows," *Journal of Computational Physics*, Vol. 225, pp. 1159-1174, 2007.
- <sup>14</sup>Titov, E.V., and Levin, D.A., "Extension of the DSMC method to high pressure flows," *International Journal of Computational Fluid Dynamics*, Vol. 21, Nos. 9-10, pp. 351-368, 2007.
- <sup>15</sup>Macrossan, M. N. and Geng, X., "Detecting Equilibrium Cells in DSMC to Improve the Computational Efficiency," *Rarefied Gas Dynamics: 25th International Symposium*, St. Petersburg, Russia, 21-28 July, 2006.
- <sup>16</sup>LeBeau, G. J., "A parallel implementation of the direct simulation Monte Carlo method," *Computer Methods in Applied Mechanics and Engineering*, Vol. 174, pp. 319-337, 1999.
- <sup>17</sup>Wu, J. S. and Tseng, K. C., "Parallel DSMC method using dynamic domain decomposition," *International Journal for Numerical Methods in Engineering*, Vol. 63, pp. 37-76, 2005.
- <sup>18</sup>Shuvalov, V. V., "Multi-dimensional hydrodynamic code SOVA for interfacial flows: Application to the thermal layer effect," *Shock Waves*, Vol. 9, pp. 381-390, 1999.
- <sup>19</sup>Stewart, B. D., Pierazzo, E., Goldstein, D. B., Varghese, P. L. and Trafton, L. M., "Simulation of Low Density Atmospheric Flow on the Moon Following a Comet Impact," *to be published*.
- <sup>20</sup>Zhang, J., Goldstein, D. B., Varghese, P. L., Gimelshein, N. E., Gimelshein, S. F. and Levin, D. A., "Simulation of gas dynamics and radiation in volcanic plumes on Io," *Icarus*, Vol. 163, pp. 182-197, 2003.
- <sup>21</sup>Pacheco, P. S., "Parallel Programming with MPI," *Morgan Kaufman Publisher*, San Francisco, pp. 41-110, 1997.
- <sup>22</sup>Sedov, L. I., "Similarity and Dimensional Methods in Mechanics," *Academic Press*, London, pp. 271-281, 1959.
- <sup>23</sup>Stanyukovich, K. P., "Unsteady Motion of Continuous Media," *Pergamon*, New York, 1960.
- <sup>24</sup>Zel'Dovich, Y. B. and Raizer, Y. P., "Physics of shock waves and high-temperature hydrodynamic phenomena," *Academic press*, New York, Vol. 2, pp. 571-584, 1967.
- <sup>25</sup>Tzuk Y., Barmashenko, B. D., Bar I., and Rosenwaks S., "The sudden expansion of a gas cloud into vacuum revisited," *Physics of Fluids A*, Vol. 5, No. 12, pp. 3265-3272, 1993.
- <sup>26</sup>VanGilder, D. B., Chartrand, C. C., Papp, J., Wilmoth, R. and Sinha, N., "Computational Modeling of Nearfield to Farfield Plume Expansion," *43rd Joint Propulsion Conference & Exhibit*, AIAA 2007-5704, Cincinnati, 2007.
- <sup>27</sup>Bird, G. A., "Breakdown of Translational and Rotational Equilibrium in Gaseous Expansions," *AIAA Journal*, Vol. 8, No. 11, pp. 1998-2003, 1970.
- <sup>28</sup>Bird, G. A., "A criterion for the breakdown of vibrational equilibrium in expansions," *Physics of Fluids*, Vol. 14, No. 5, pp. 1732-1735, 2002.
- <sup>29</sup>Bykov, N. Y., Lukyanov, G. A., Bulgakov, A. V. and Bulgakova, N. M., "Modeling of Vapor Expansion under Pulsed Laser Ablation: Time-of-flight Data Analysis," *Rarefied Gas Dynamics: 24<sup>th</sup> International Symposium*, pp. 373-378, 2005.
- <sup>30</sup>Pierazzo, E. and Melosh, H. J., "Hydrocode modeling of Chicxulub as an oblique impact event," *Earth and Planetary Science Letters*, Vol. 165, pp. 163-176, 1999.
- <sup>31</sup>Pierazzo, E. and Melosh, H. J., "Hydrocode modeling of oblique impacts: the fate of the projectile," *Meteorit. Planet. Sci.*, Vol. 35, No. 1, pp. 117-130, 2000.